Open heavy-flavour measurements at forward rapidity via semi-muonic decays with ALICE at the LHC

Maolin Zhang (maolin.zhang@cern.ch)

Laboratoire de Physique Clermont Auvergne, UCA, France
Institute Of Particle Physics, CCNU, China

Outline
- ❖ Motivations
- ❖ The ALICE detector
- ❖ Latest measurements
- ❖ Run 3 perspectives

15th FCPPN/L Workshop
10-14, June, 2024,Bordeaux, FRANCE

Physics motivations

Heavy (charm and beauty) quarks: sensitive probes of the quark-gluon plasma (QGP)

- $\tau_{c/b}$ ~ 0.01-0.1 (fm/*c*) < τ_{QGP} ~0.3 (fm/*c*) [PRC 89 (2014) 034906]
- Experience the whole collision evolution

❖ Key observable: azimuthal anisotropy quantified by means of a Fourier expansion of azimuthal distributions of produced particles

$$\frac{dN}{d\varphi} \propto 1 + \sum_{n=1}^{\infty} 2v_n \cos[n(\varphi - \Psi_n)]$$

$$v_n = <\cos n(\varphi - \Psi_n)>$$
$$n = 2, \text{elliptic flow}$$

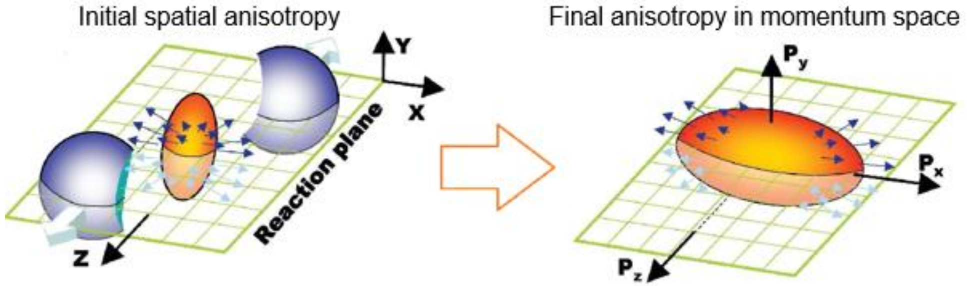

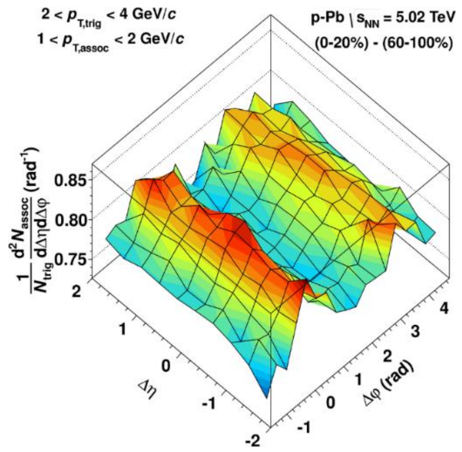

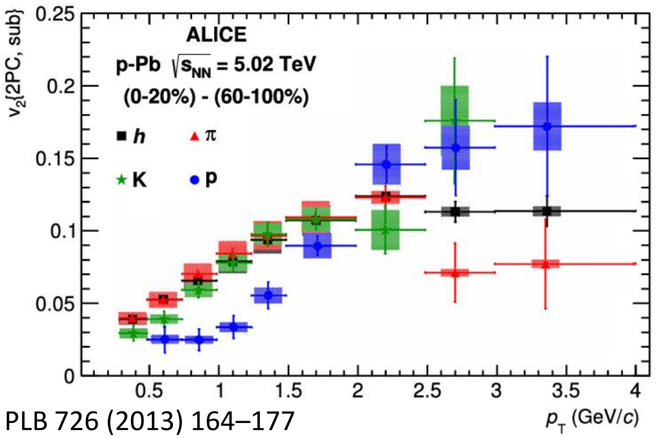

PLB 726 (2013) 164–177

Small collision systems (pp & p–Pb collisions):

❖ Baseline for heavy-ion collisions
❖ pp collisions: test pQCD-based calculations and production mechanisms
❖ p–Pb collisions: cold nuclear matter effects and study of nuclear parton distribution functions

No (or very tiny) QGP effect is expected

❖ Long-range angular correlations and clear mass ordering observed in p–Pb collisions at high multiplicity, as in Pb–Pb collisions

The ALICE detector (Run 2 layout)

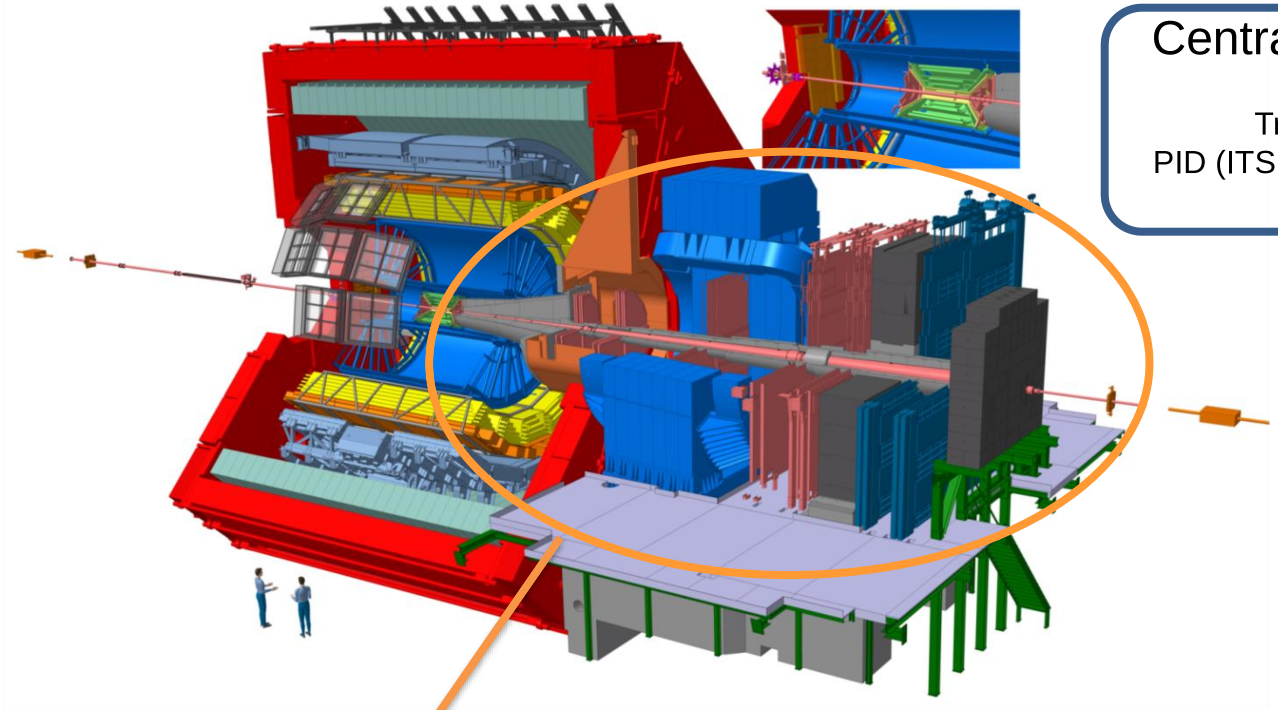

Central Barrel, $|\eta| < 0.9$

Vertexing (ITS),
Tracking (ITS, TPC),
PID (ITS, TPC, TOF, TRD, HMPID, Calorimeters)

Forward/ Backward detectors (V0, T0, ZDC):

Trigger,
Timing,
Multiplicity/ Centrality,
Event plane

Muon spectrometer
$-4 < \eta < -2.5$

Tracking,
Triggering,
μ identification

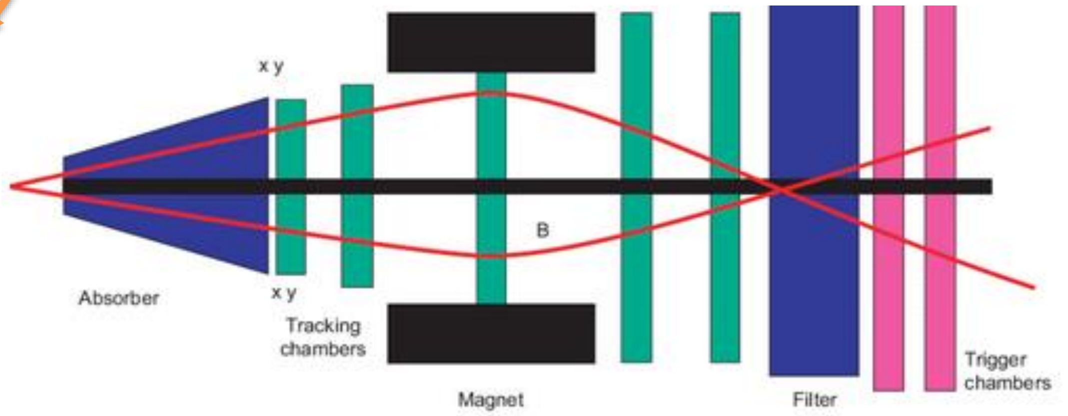

Int. J. Mod. Phys. A29 (2014) 1430044

Hadronic decays ($|y| < 0.8$)

- $D^0 \to K^-\pi^+$
- $D^+ \to K^-\pi^+\pi^+$
- $D^{*+} \to D^0 (\to K^-\pi^+)\ \pi^+$
- $D^+_s \to \phi\ (\to K^-K^+)\pi^+$
- $D_{s1}{}^+ \to D^{*+} K^0_s$
- $D_{s2}{}^{*+} \to D^+ K^0_s$
- $\Lambda_c{}^+ \to pK^0_s,\ \Lambda_c{}^+ \to pK^-\pi^+$
- $\Lambda_c{}^+ \to e^+\Lambda\nu_e$
- $\Xi_c{}^0 \to e^+\Xi^-\nu_e,\ \Xi_c{}^0 \to \pi^+\Xi^-$
- $\Xi_c{}^+ \to \pi^+\pi^+\Xi^-$
- $\Omega_c{}^0 \to \Omega^-\pi^+$
- $\Sigma_c{}^{0,++}(2455) \to \Lambda_c{}^+\pi^{-,+}$
- $\Sigma_c{}^{0,++}(2520) \to \Lambda_c{}^+\pi^{-,+}$

Semi-leptonic decays

- **c, b $\to \mu^\pm$ ($2.5 < y < 4.0$)**
- c, b $\to e^\pm$ ($|y| < 0.8$ or 0.6

Heavy-flavour hadron decay muon v_2 in p–Pb collisions

p-going

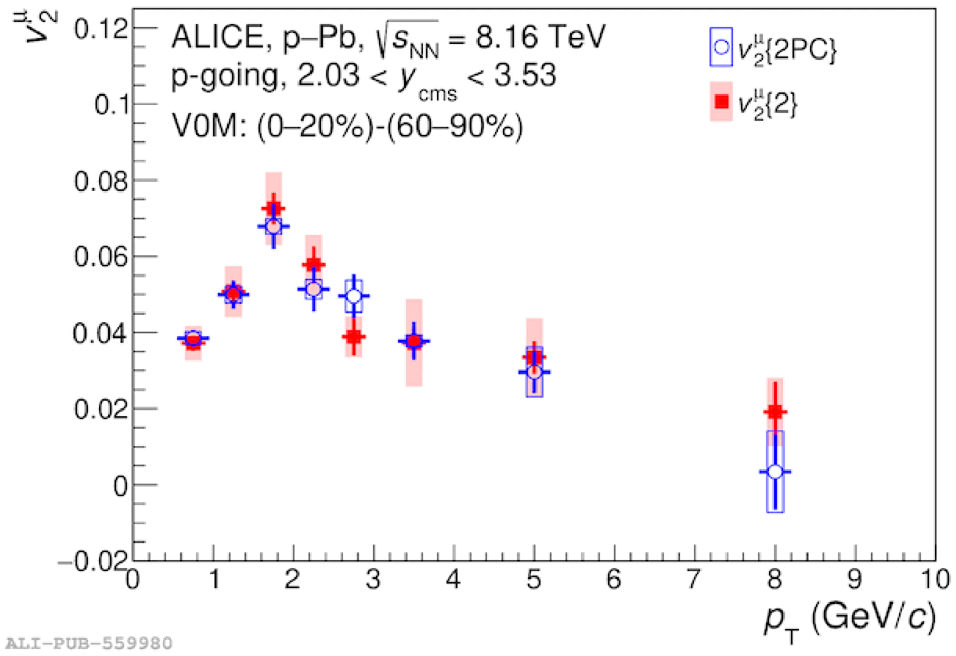

Pb-going

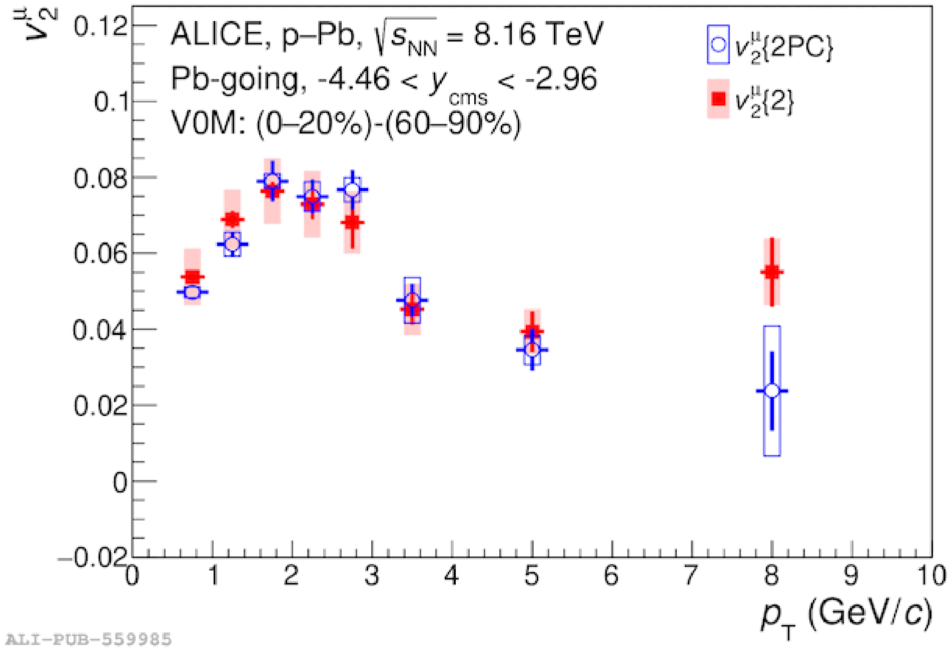

HF-μ dominate at p_T > 2 GeV/*c*

PLB 846 (2023) 137782

- ❖ Two different techniques: forward-central two-particle correlations and two-particle cumulants

- ❖ Positive muon v_2 measured for the first time over a wide p_T interval at both forward and backward rapidities with a significance of 4.7σ and 7.6σ for 2 < p_T < 6 GeV/*c*, respectively
- ❖ Consistent v_2 values with two-particle correlations and two-particle cumulants
- ❖ Hint for a smaller v_2 at forward than backward rapidity: consequence of decorrelation effects of flow vectors in different rapidity regions

Comparison with other published measurement

p-going

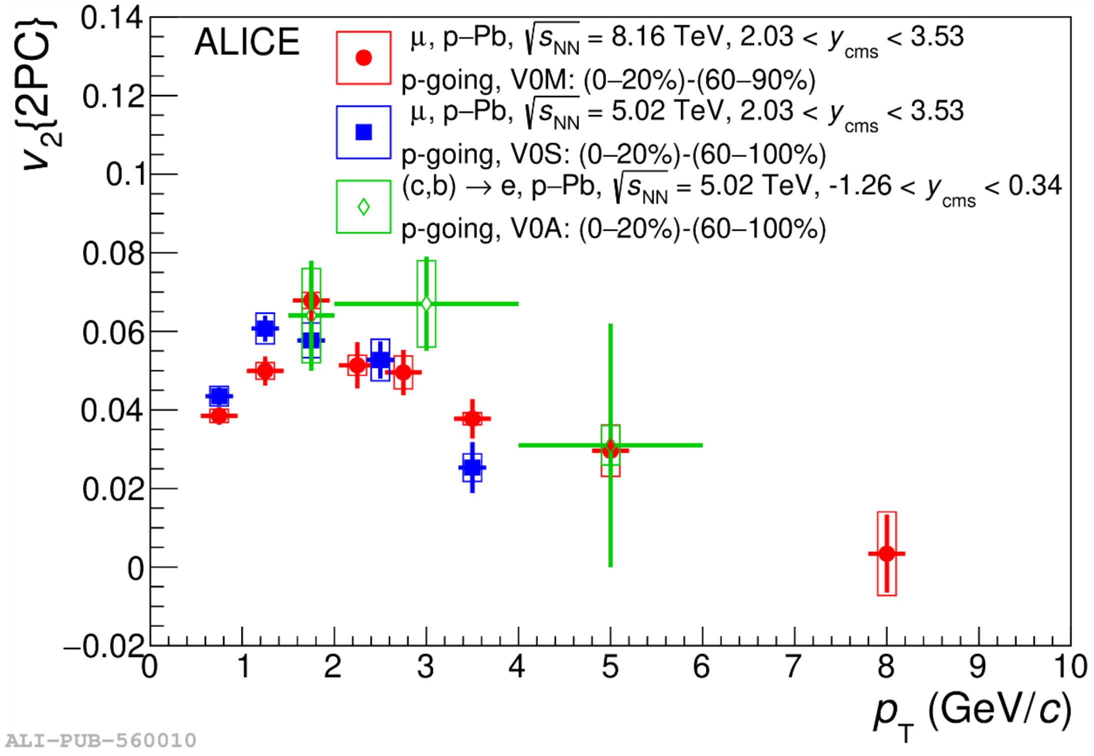

Pb-going

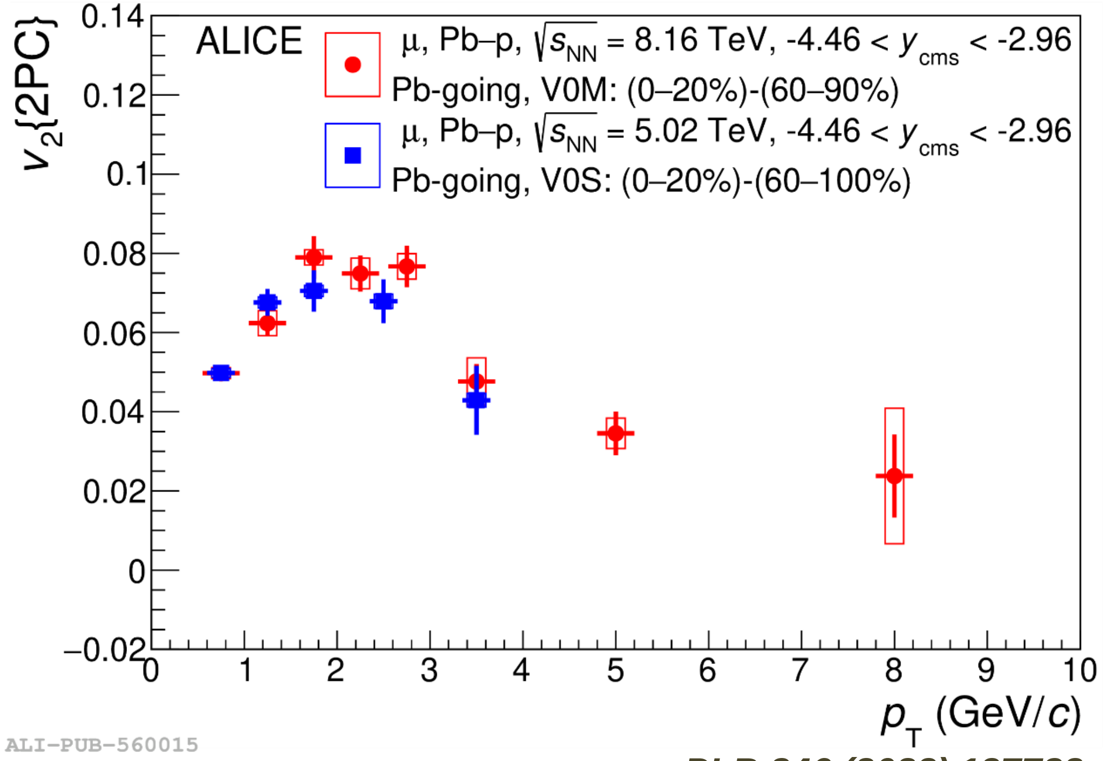

PLB 846 (2023) 137782

- No significant energy dependence on the muon v_2 values obtained at $\sqrt{s_{NN}}$ = 5.02 TeV and 8.16 TeV
- Results in good agreement within uncertainties at midrapidity with the heavy-flavour hadron decay electron v_2 at $\sqrt{s_{NN}}$ = 5.02 TeV

Comparisons with AMPT calculations

p-going

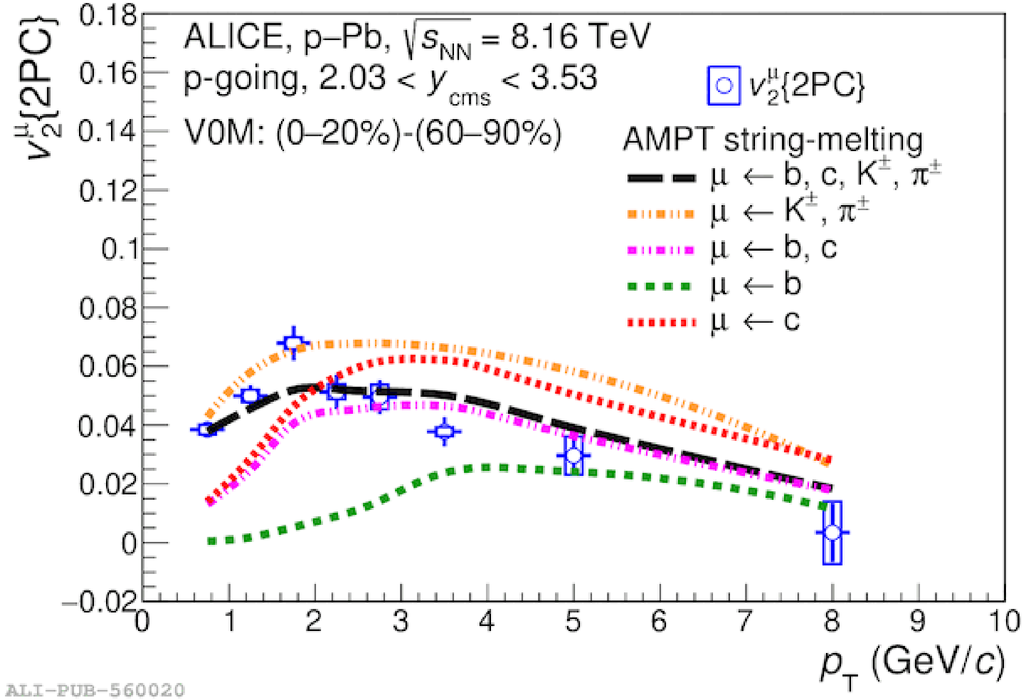

Pb-going

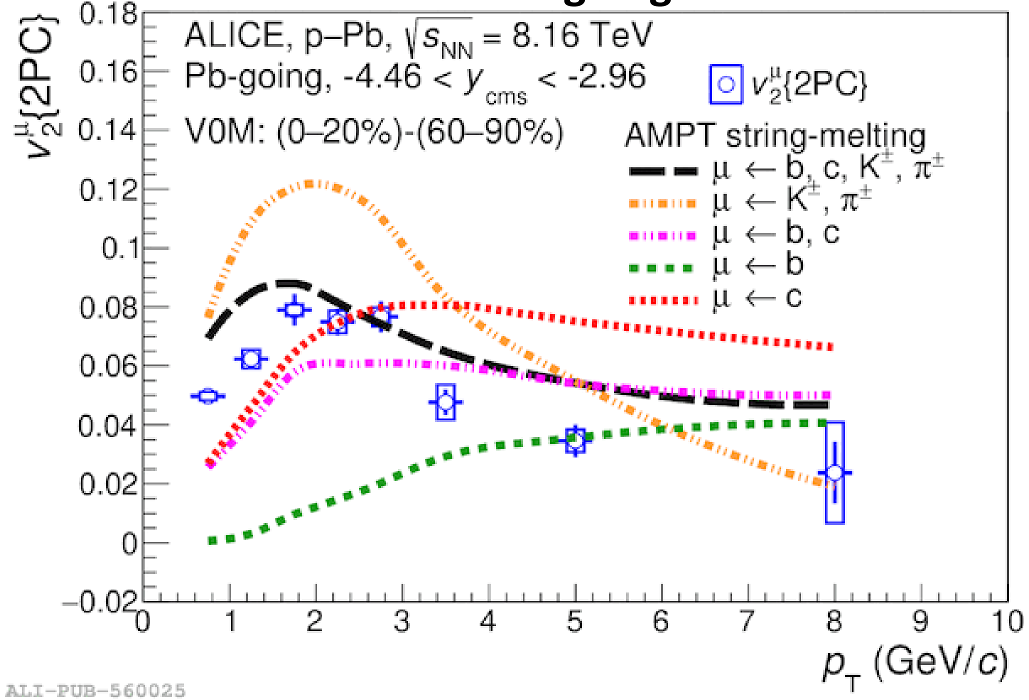

PLB 846 (2023) 137782

- AMPT calculations [Z. W. Lin, PRC 72 (2005) 064901]: non-equilibrium dynamics, microscopic evolution of parton interactions
  - Larger v_2 for muons from light-flavor hadron decays than for heavy-flavor hadron decay muons
  - Larger v_2 at backward rapidities: rapidity-dependent flow-vector fluctuations
- AMPT predictions in fair agreement with the measured v_2, although the model slightly overestimates the data at backward rapidities
  - Suggests that the v_2 could be due to the anisotropic parton escape mechanism

Comparisons with AMPT and CGC calculations

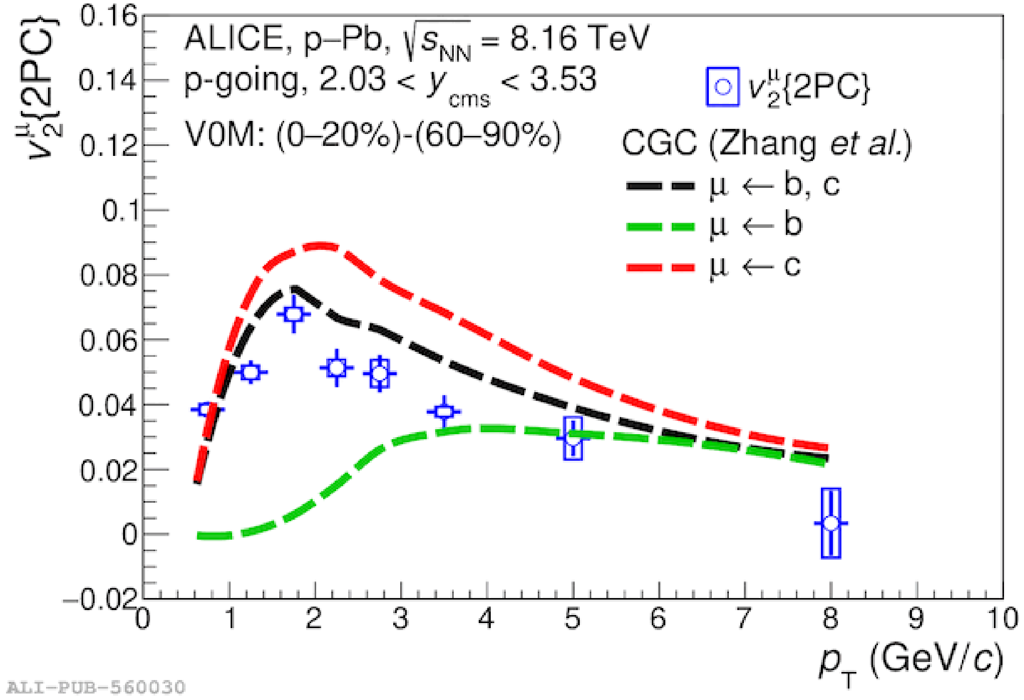

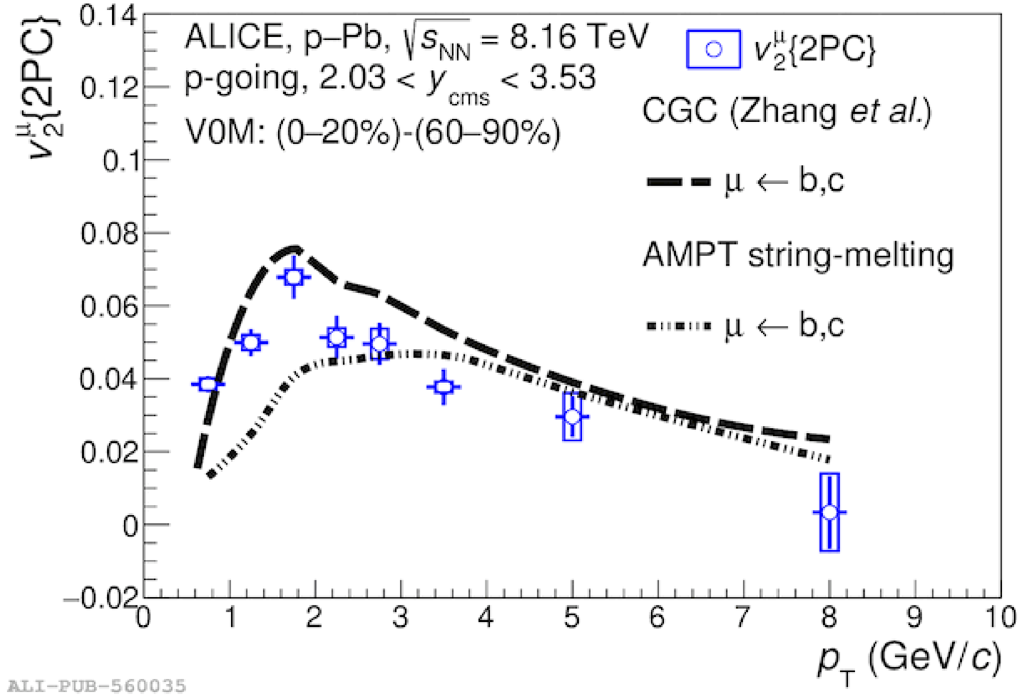

HF-μ dominate at p_T = 2 GeV/*c*

PLB 846 (2023) 137782

❖ CGC calculations [C. Zhang et al., PRL 122 (2019) 172303]: anisotropy generated from parton interactions in the early stage of collisions

- Qualitative agreement with the measured v_2
- Larger v_2 for heavy-flavour hadron decay muons at low p_T compared to AMPT
- Compatible v_2 at high p_T with AMPT: heavy-flavour dominate
- Possible contributions from initial-state effects not fully excluded

Heavy-flavour production in pp collisions at forward y via $\mu^+\mu^-$

- Charm and beauty production measured at $2.5 < y < 4.0$ in pp collisions at $\sqrt{s}$ = 13 TeV, exploiting the dimuon high-mass continuum dominated by the semimuonic decays of heavy-flavour hadrons
- Simultaneous fit to the mass and p_T distributions with a combined template of the main sources in the continuum
  - Templates extracted from the heavy-flavour enriched PYTHIA 8 simulations

PYTHIA 8: Comput. Phys. Commun. 191 (2015) 159

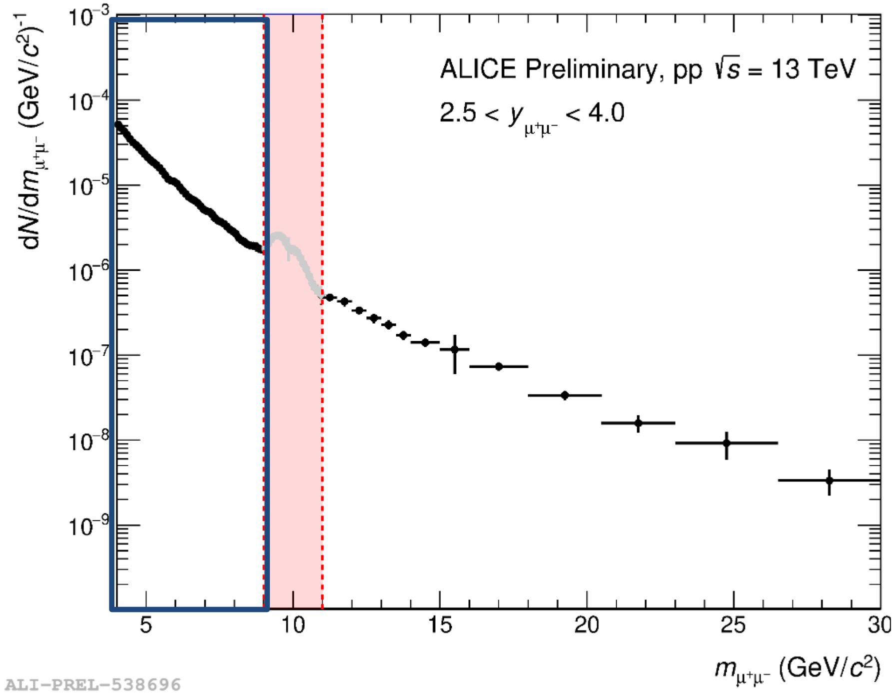

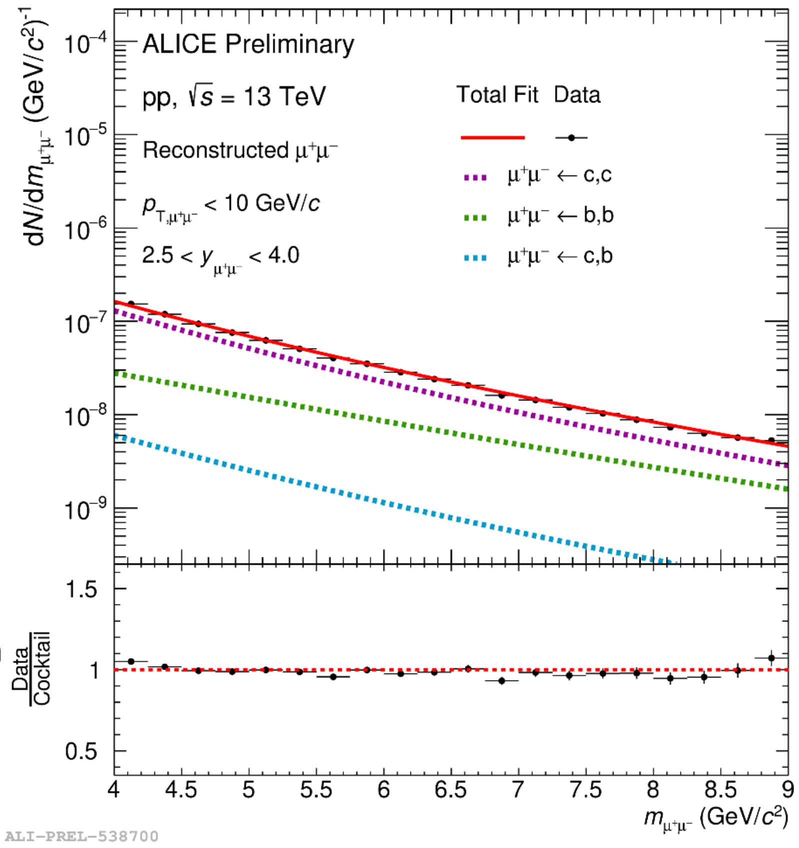

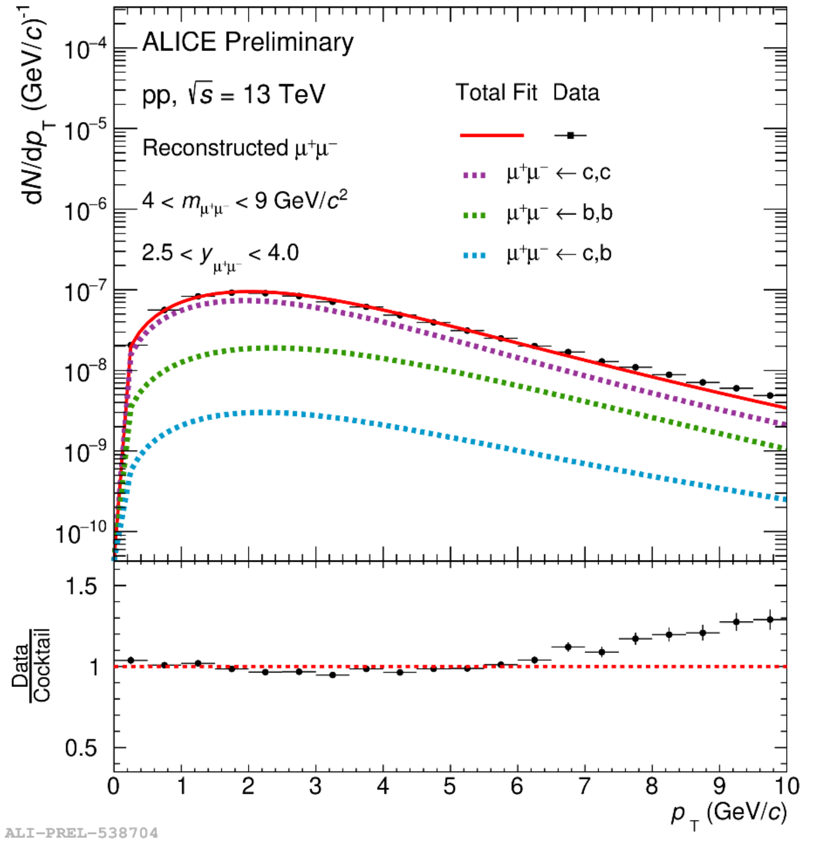

Charm and beauty production cross sections at forward y in pp collisions at $\sqrt{s}$ = 13 TeV

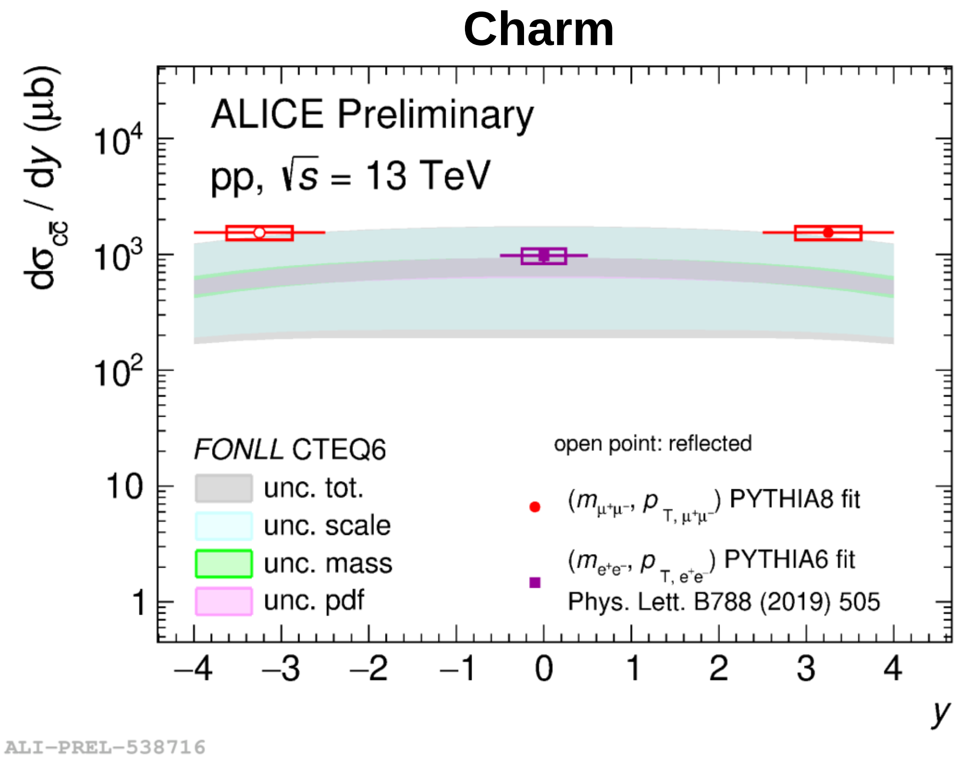

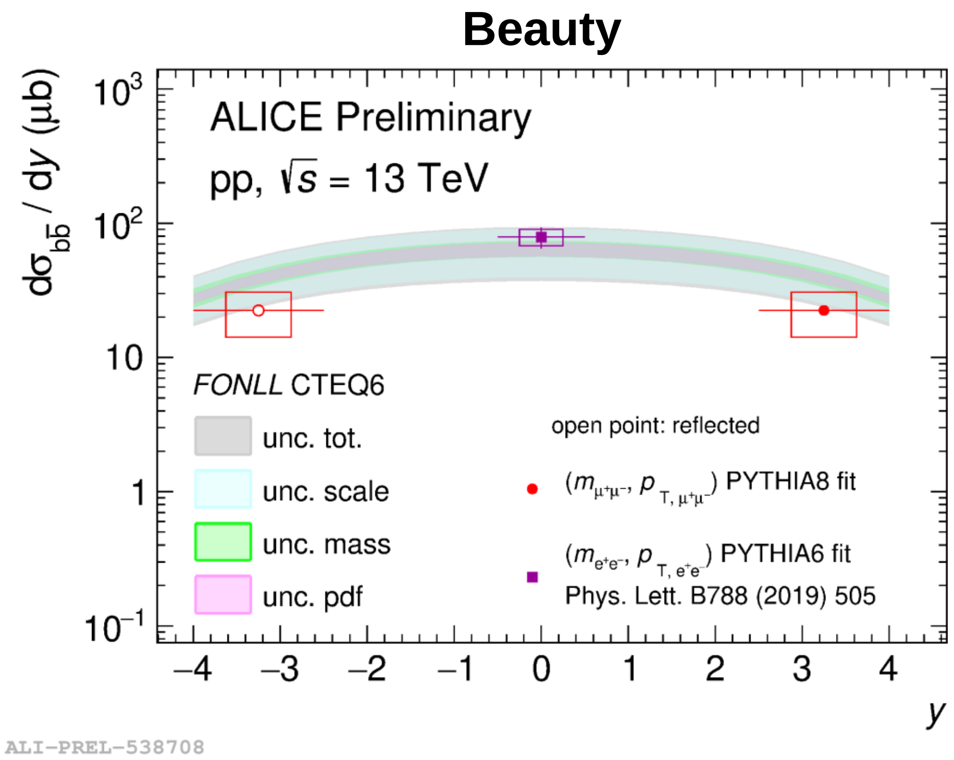

- Charm and beauty production cross sections measured separately at forward rapidity via the dimuon continuum
- Results in agreement with FONLL predictions within uncertainties, although they lie at the upper and lower limit of the calculations for charm and beauty production cross section, respectively
- Complement the previously published results at midrapidity in the dielectron channel

FONLL: JHEP 05 (1998) 007

The ALICE detector: Run 3 setup

- ❖ Major upgrades installed in 2019-2021
- ❖ Data taking started at mid 2022

New GEM-based TPC

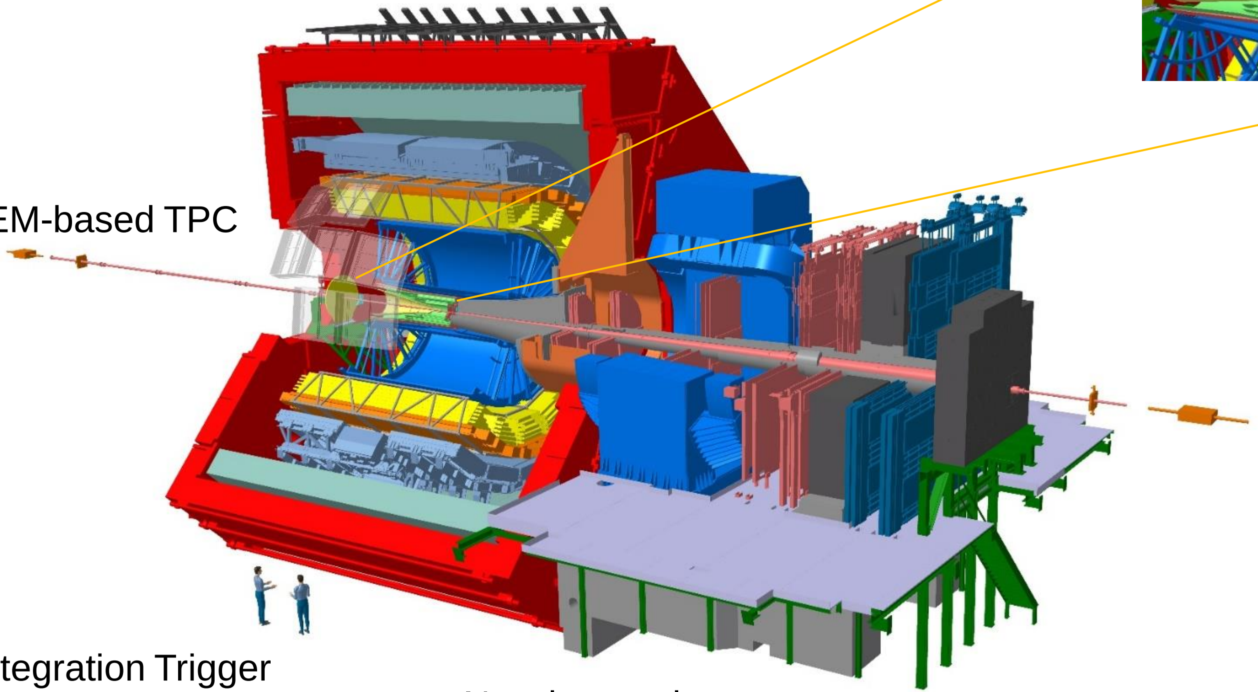

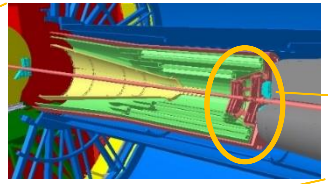

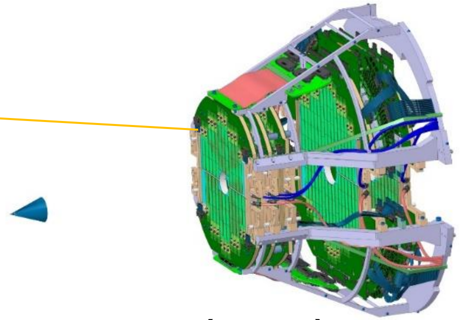

MFT

Fast Integration Trigger

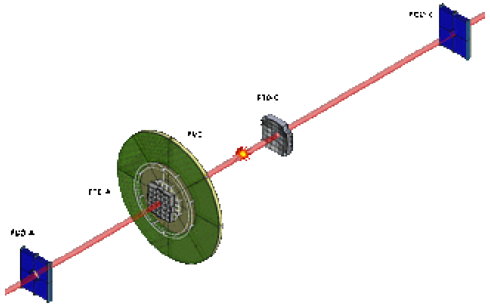

New beam pipe

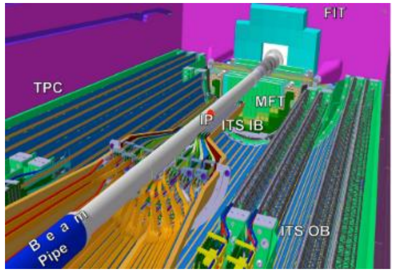

- ❖ New Inner Tracking System (ITS2)
  - Better pointing resolution at midrapidity
- ❖ New Muon Forward Tracker (MFT)
  - Vertexing also at forward rapidity ($-3.6 < \eta < -2.5$)
  - Separation of charm and beauty components in the single muon channel at forward rapidity for the first time
- ❖ New readout system of most subdetectors
  - Continuous readout and increased luminosity
  - Multidifferential measurements of various muon sources down to lower p_T and up to higher p_T
- ❖ Extend heavy flavour measurements towards the forward rapidity region allowing for c/b separation

Midrapidity: non-prompt D^0-meson fraction in pp collisions at $\sqrt{s}$ =13.6 TeV

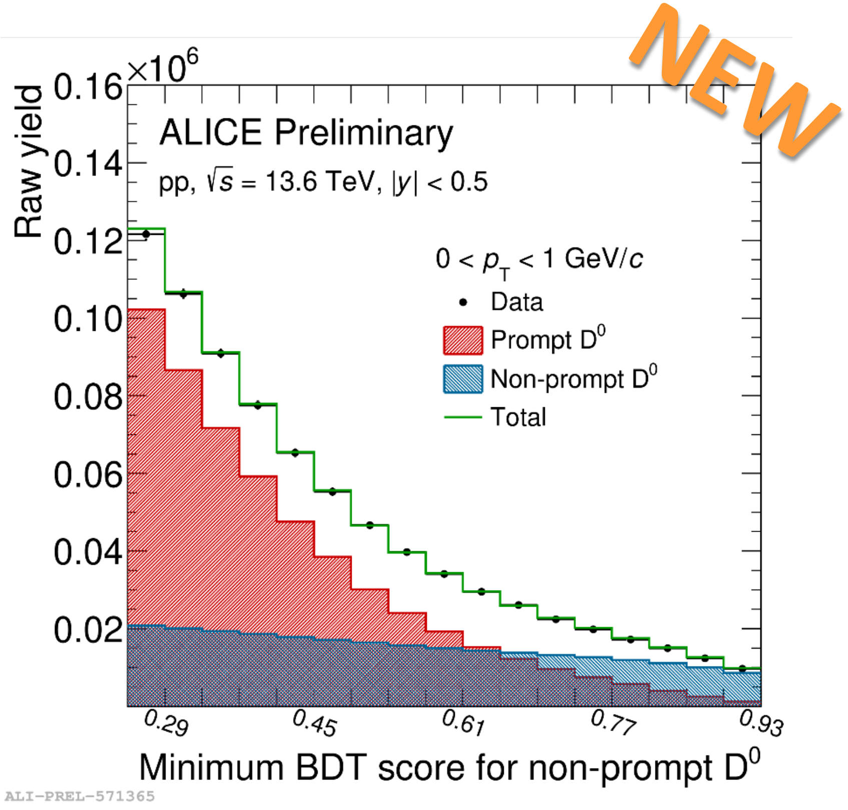

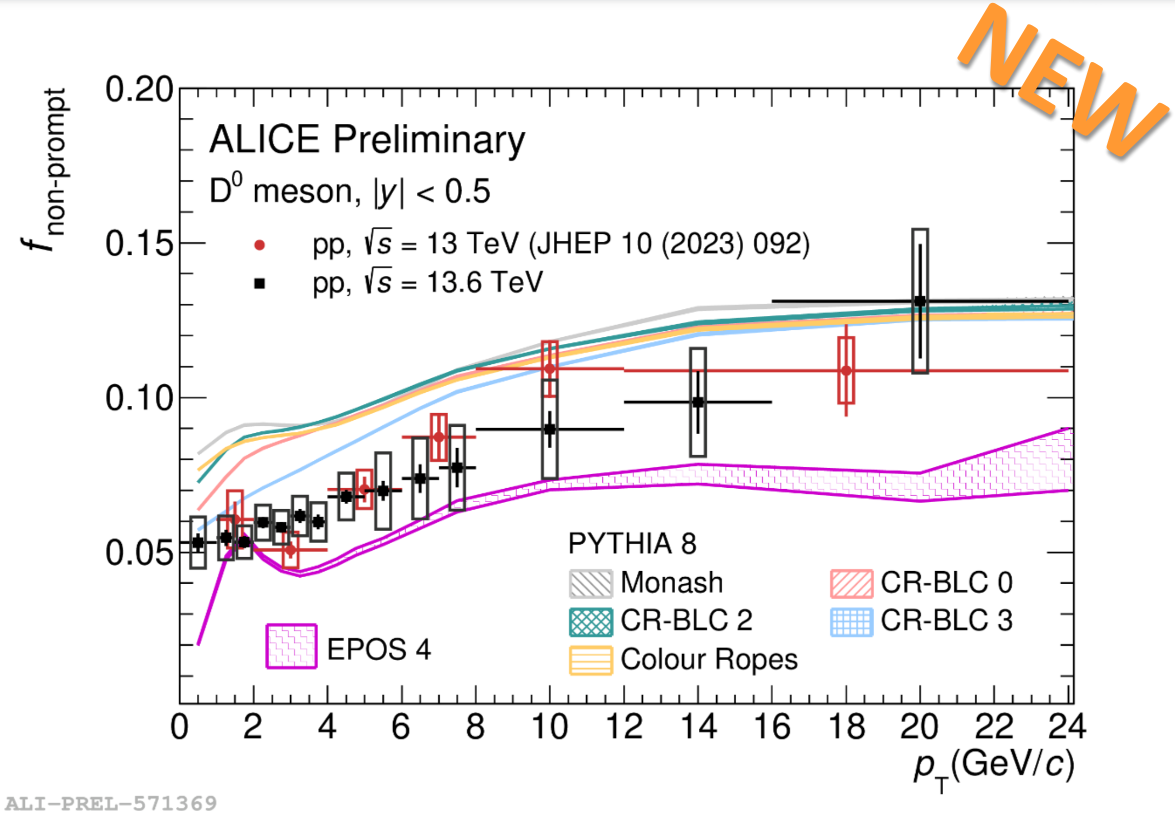

- First measurement of the non-prompt D^0-meson fraction down to p_T = 0 in Run 3
  - In agreement with the measurements in pp collisions $\sqrt{s}$ = 13 TeV
  - Increased granularity and extended p_T reach
  - Strong constraints on model calculations

Open heavy-flavour measurements via single muons in Run 3

- High p_T region measurements feasible even with a fraction of the 2022-2023 pp sample at $\sqrt{s}$ = 13.6 TeV
- Muons from W-boson decays clearly observed at p_T ~ 40 GeV/c
- Very promising to perform multidifferential measurements of open heavy flavours in the semimuonic channel with high precision, analysing the full pp sample

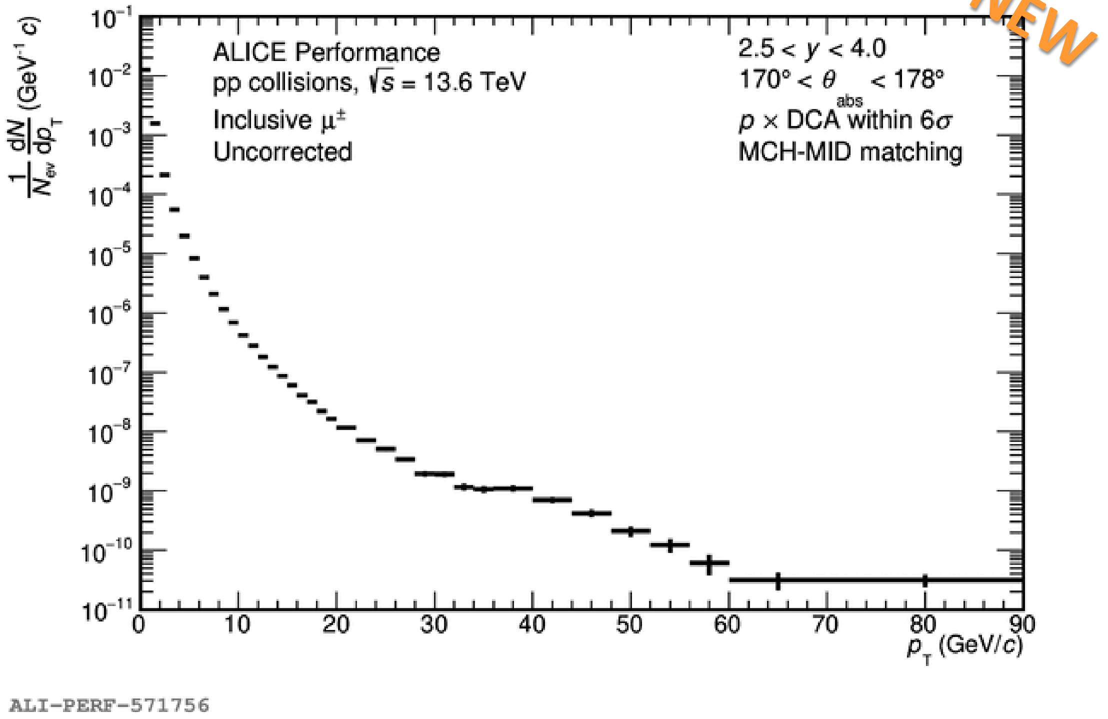

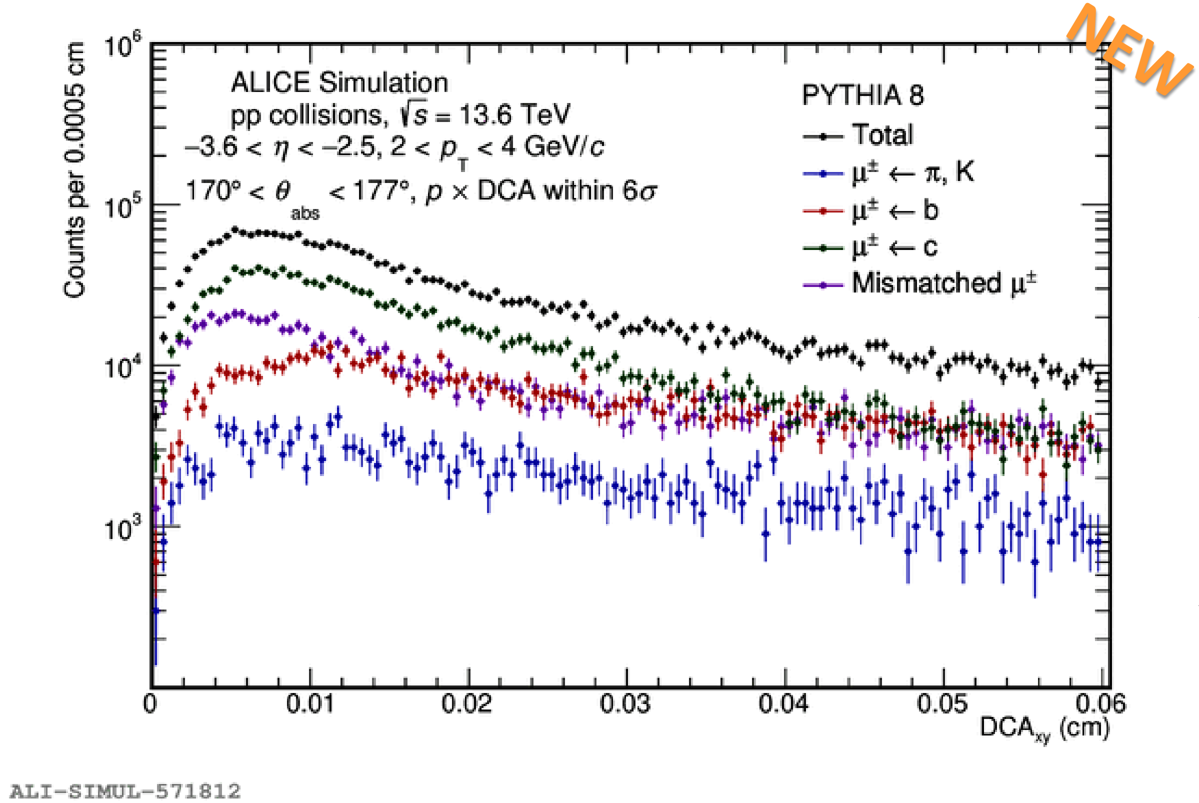

- Different decay length of charm and beauty hadrons
  - Observable: DCA_{xy} (Distance of Closest Approach to the primary vertex in the transverse plane) of heavy-flavour decay muons

- Distinct features of various sources: charm and beauty separation at forward rapidity can be achieved with the MFT

Strategy to separate charm- and beauty-decay muons

- Procedure based on Monte Carlo templates of DCA_{xy} for each source and in each p_T interval
  - Parametrized with a variable-width Gaussian function
  - Total DCA_{xy} distribution for each p_T interval fitted as a combination of the various templates
  - Closure test performed varying fit parameters to mimic detector effects

- Procedure validated with full realistic simulations

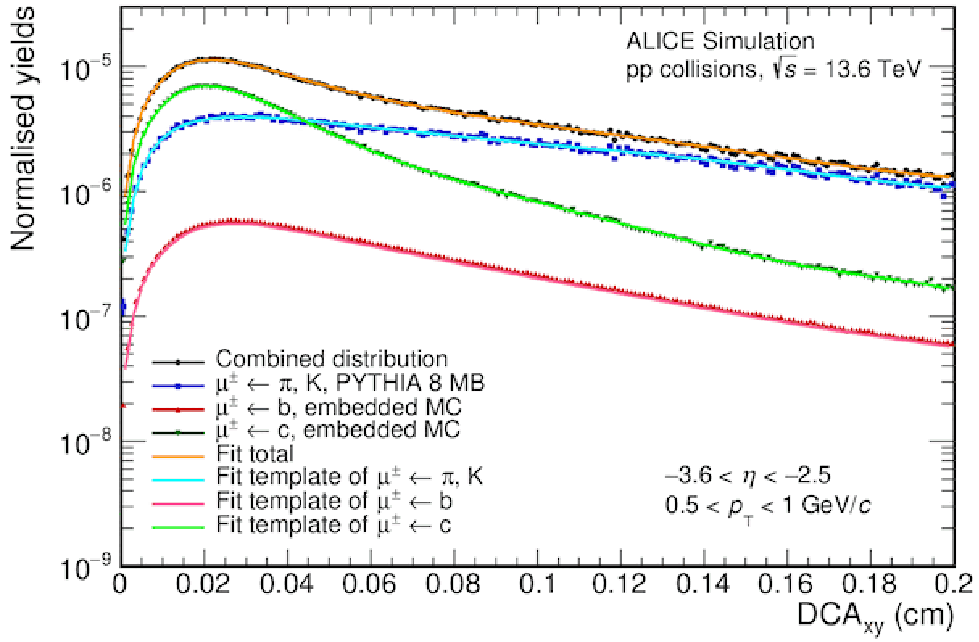

ALI-SIMUL-547324

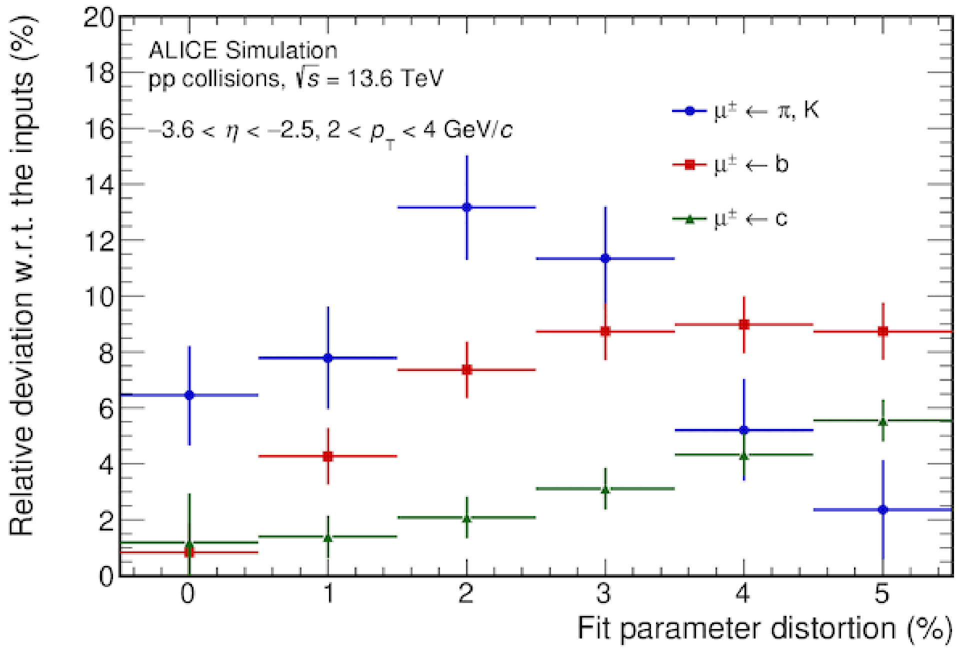

ALI-SIMUL-547377

- μ ← c and μ ← b can be measured separately in the semimuonic channel at forward rapidity in pp collisions at $\sqrt{s}$ = 13.6 TeV with the MFT coupled with the muon spectrometer, **down to the low p_T region**

Conclusion

- Azimuthal anisotropies in small collision systems
  - Collective-like behaviour of heavy quarks in high-multiplicity p–Pb collisions at both forward and backward rapidities
  - New constraints in the interpretation of the collective-like behaviour in small collision systems and to the model calculations

- p_{T} -integrated production cross section of charm and beauty measured via dimuons in pp collisions at $\sqrt{s}$ = 13 TeV

- The Muon Forward Tracker allows us to inquire further physics channels
  - Multidifferential measurements of production of charm- and beauty-decay muons separately in the semimuonic channel down to low p_{T}
  - Template fit method tested and validated with full Monte Carlo simulations

Stay tuned: more to come soon in both pp and Pb–Pb collisions for the measurements in the semimuonic channel

Thank you for your listening!

BACKUP SLIDES

Backup slides: AMPT(A multiphase transport) model

- **Initial conditions:** HIJING two-component model
- **String melting:** hadrons from string fragmentation are melted into primordial quarks and antiquarks
  - Quark formation time: $t_{\mathrm{f}} = E_{\mathrm{H}}/m^2_{\mathrm{T,H}}$
- **Parton cascade:** two-body elastic scattering described by ZPC model

Debye screening mass

$$\frac{d\sigma}{dt} = \frac{9\pi\alpha_s^2}{2}\left(1+\frac{\mu^2}{s}\right)\frac{1}{(t-\mu^2)^2}$$

- **Coalescence:** combine nearest quarks to meson/baryon
- **A Relativistic Transport (ART)** to describe hadron scatterings

Structure of AMPT v2.xx (String Melting Version)

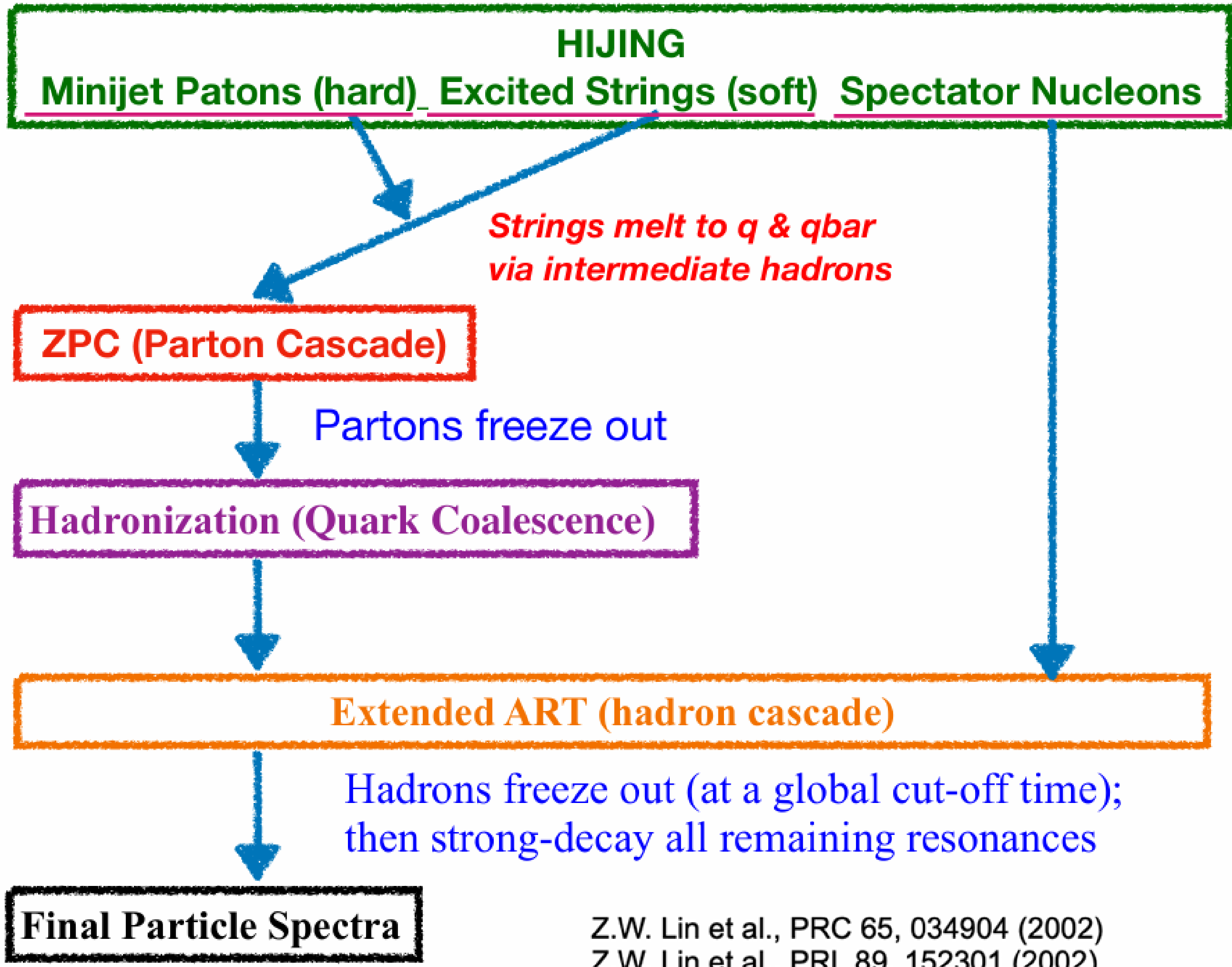

Z.W. Lin et al., PRC 65, 034904 (2002)
Z.W. Lin et al., PRL 89, 152301 (2002)

Backup slides: escape mechanisms

Zi-Wei Lin, IHEP2016

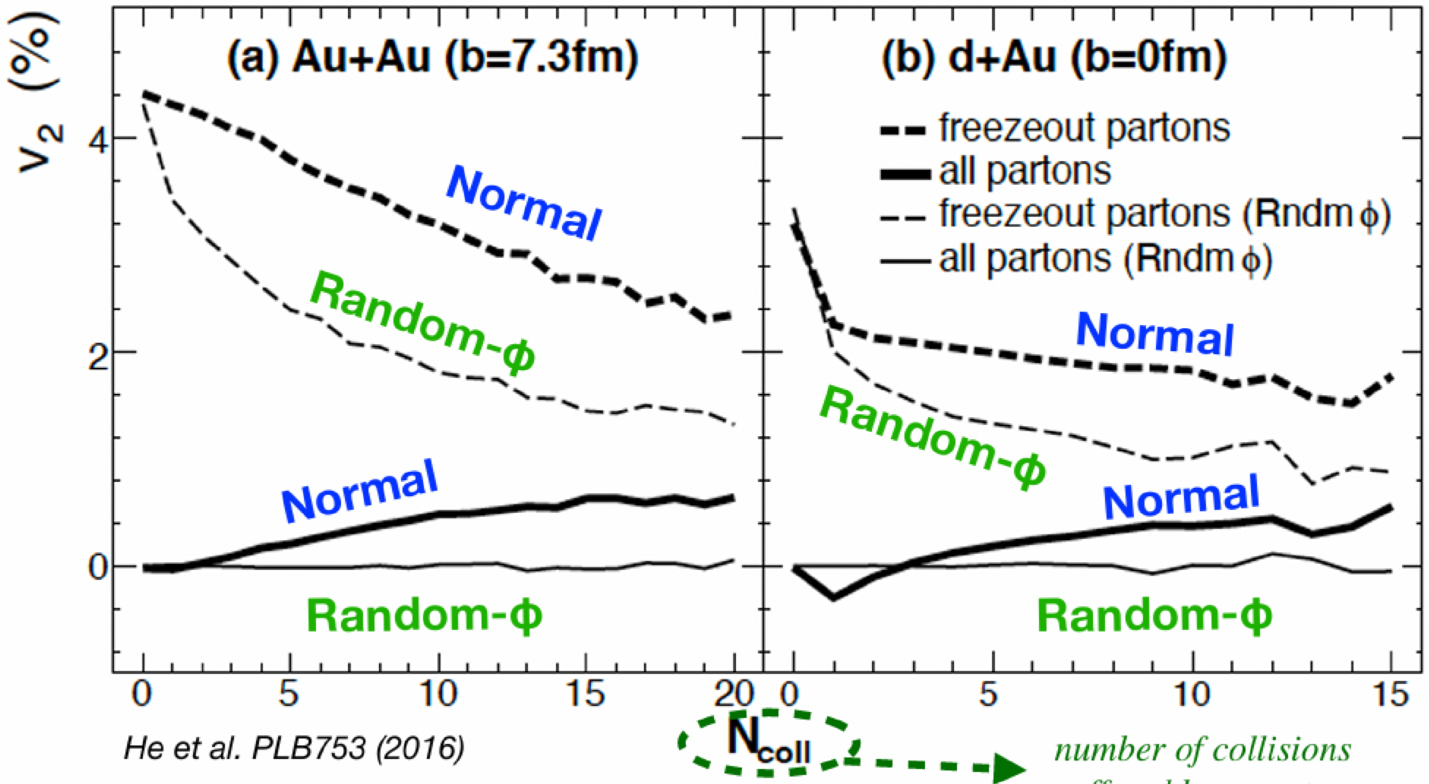

He et al. PLB753 (2016)

number of collisions suffered by a parton

Freeze out partons: freeze out after exactly N_{coll} collisions;

Active partons: will collide further, freeze out after > N_{coll};

All partons: sum of the above two partons

v_2	Normal v_2	Random-ϕ v_2
Au+Au	3.9%	2.7%
d+Au	2.7%	2.5%

	Fraction from pure escape	$\langle N_{coll}\rangle$ all partons
Au+Au	69%	4.6(modest)
d+Au	93%	1.2(low)

Normal:

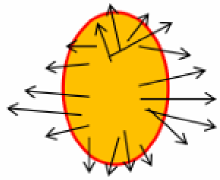

Random:

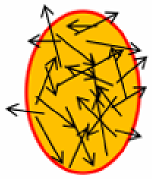

- Few interactions are sufficient for anisotropy in AMPT
  - Partons more likely to escape in the short direction
  - Particle escape is the dominant mechanism for v_2 in small collision systems
  - The v_2 from pure escape decrease with increasing N_{coll} → transport approach hydrodynamics

Backup slides: nonflow subtraction

ALICE

- The nonflow contribution is estimated in low-multiplicity (60–90%) events, and subtracted for both differential and reference cumulants

$$v_2^{\mu}\{2\}(p_{\mathrm{T}}) = \frac{[d_2^{\mu}\{2\}(p_{\mathrm{T}})]_{(0-20\%)}}{\sqrt{[c_2\{2\}]_{(0-20\%)}}}$$

subtraction of long-range jet correlation

$$v_2^{\mu}\{2\}(p_{\mathrm{T}}) = \frac{[d_2^{\mu}\{2\}(p_{\mathrm{T}})]_{(0-20\%)} - f\cdot[d_2^{\mu}\{2\}(p_{\mathrm{T}})]_{(60-90\%)}}{\sqrt{[c_2\{2\}]_{(0-20\%)} - f\cdot[c_2\{2\}]_{(60-90\%)}}}$$

subtraction of remains long-range and short-range jet correlation

$$v_2^{\mu}\{2\}(p_{\mathrm{T}}) = \frac{[d_2^{\mu}\{2\}(p_{\mathrm{T}})]_{(0-20\%)} - f\cdot f'\cdot[d_2^{\mu}\{2\}(p_{\mathrm{T}})]_{(60-90\%)}}{f_{\mathrm{RP}}\cdot\sqrt{[c_2\{2\}]_{(0-20\%)} - f\cdot[c_2\{2\}]_{(60-90\%)}}}\cdot f_{\Delta\eta}$$

f : the ratio of mean SPD tracklet in low-multiplicity collisions to that in high-multiplicity collisions

f_{RP}, f' : the factors to remove the **remaining long-range jet correlations**, obtained from two-particle correlations

$f_{\Delta\eta}$: the factor to suppress the **short-range jet correlations**

Backup slides: non-prompt D^0-meson fraction

Define n sets of selections with different prompt and non-prompt D^0 contributions

For each selection set, the raw yield and the efficiencies are related to the corrected yields of prompt N_{prompt} and non-prompt $N_{non-prompt}$ D^0

$$\begin{cases} (\text{Acc} \times \epsilon)_1^{prompt} \cdot N_{prompt} + (\text{Acc} \times \epsilon)_1^{non-prompt} \cdot N_{non-prompt} = Y_1 \\ \dots \\ (\text{Acc} \times \epsilon)_n^{prompt} \cdot N_{prompt} + (\text{Acc} \times \epsilon)_n^{non-prompt} \cdot N_{non-prompt} = Y_n \end{cases}$$

The algebraic equations can be represented by:

$$\begin{pmatrix} \varepsilon_1^{\mathrm{p}} & \varepsilon_1^{\mathrm{np}} \\ \vdots & \vdots \\ \varepsilon_n^{\mathrm{p}} & \varepsilon_n^{\mathrm{np}} \end{pmatrix} \times \begin{pmatrix} N_{\mathrm{p}} \\ N_{\mathrm{np}} \end{pmatrix} - \begin{pmatrix} Y_1 \\ \vdots \\ Y_n \end{pmatrix} = \begin{pmatrix} \delta_2 \\ \vdots \\ \delta_n \end{pmatrix}$$

The χ^2 of the system is defined as:

$$\chi^2 = \delta^T C^{-1} \delta \,,$$

where C is the covariance matrix from the uncertainties

Corrected yields of prompt and non-prompt D^0 obtained from χ^2 minimization of the system

Non-prompt fraction $f_{non-prompt}$ evaluated for a given set of selections as

$$f^i_{non-prompt} = \frac{(\text{Acc} \times \epsilon)_i^{non-prompt} \cdot N_{non-prompt}}{(\text{Acc} \times \epsilon)_i^{non-prompt} \cdot N_{non-prompt} + (\text{Acc} \times \epsilon)_i^{prompt} \cdot N_{prompt}}$$

Backup slides

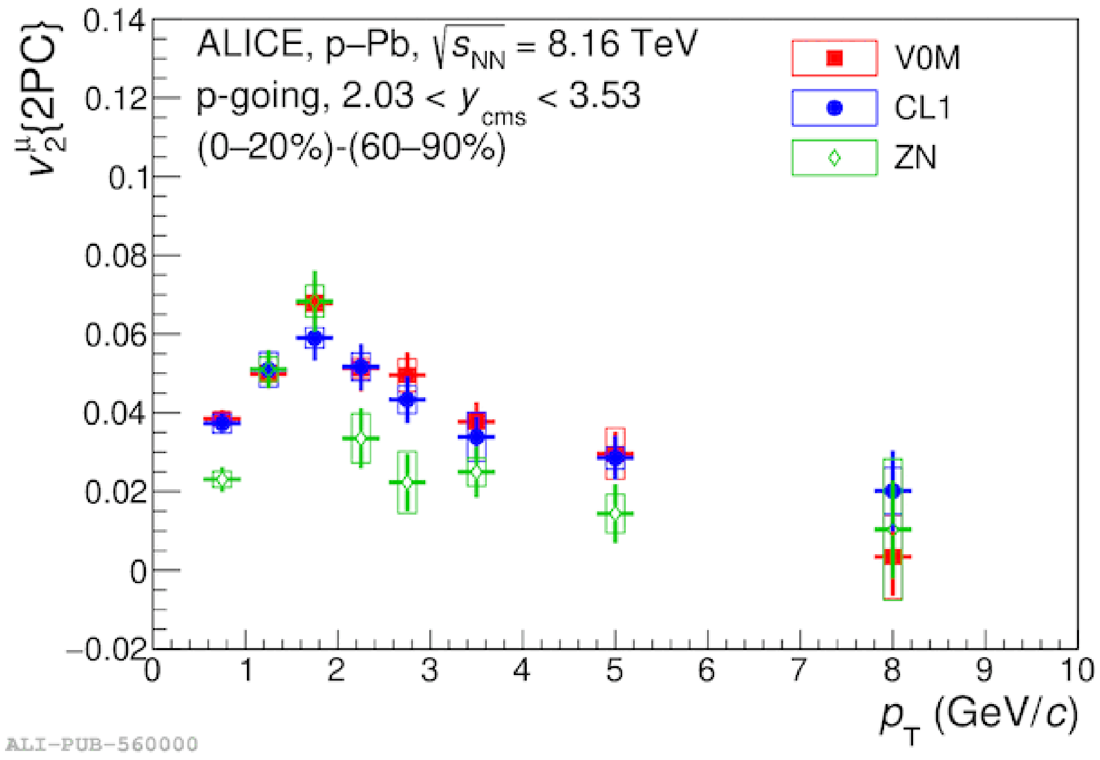

❖ Compatible v_2 values with different multiplicity estimators within uncertainties with a hint for a smaller v_2 using the energy deposited in the neutron ZDC

Strategy to separate charm- and beauty-decay muons

- Procedure based on Monte Carlo templates of DCA_{xy} for each source and in each p_T interval
  - Parametrized with a variable-width Gaussian function, the width being a polynomial function of the DCA_{xy}

$$f(x) = Ae^{-(x-\mu)^2/2\sigma(x)^2}$$
$$\sigma(x) = \sigma_0^L + \sigma_1^L(\mu - x) + \ldots + \sigma_3^L(\mu - x)^3 \text{ for } x \leq \mu$$
$$\sigma(x) = \sigma_0^R + \sigma_1^R(x - \mu) + \ldots + \sigma_6^R(x - \mu)^6 \text{ for } x > \mu$$

  - Total DCA_{xy} distribution for each p_T interval fitted as a combination of the various templates

$$f(x) = B \cdot f_b(x) + C \cdot f_c(x) + D \cdot f_{bkg}(x)$$

  - Extraction of yields of $\mu \leftarrow c$ and $\mu \leftarrow b$

Strategy to separate charm- and beauty-decay muons

- Closure test: varying fit parameters to mimic detector effects
  - Randomly vary width parameters by 1% to 5% to generate distorted templates
  - Refit DCA_{xy} using these distorted templates and examine the sensitivity through their relative deviations

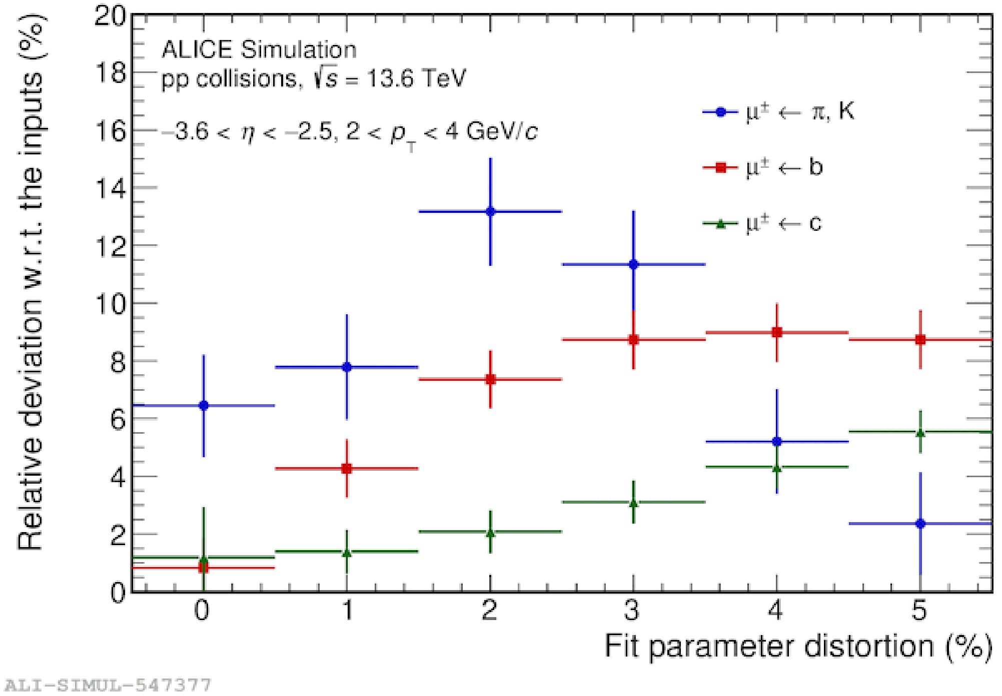

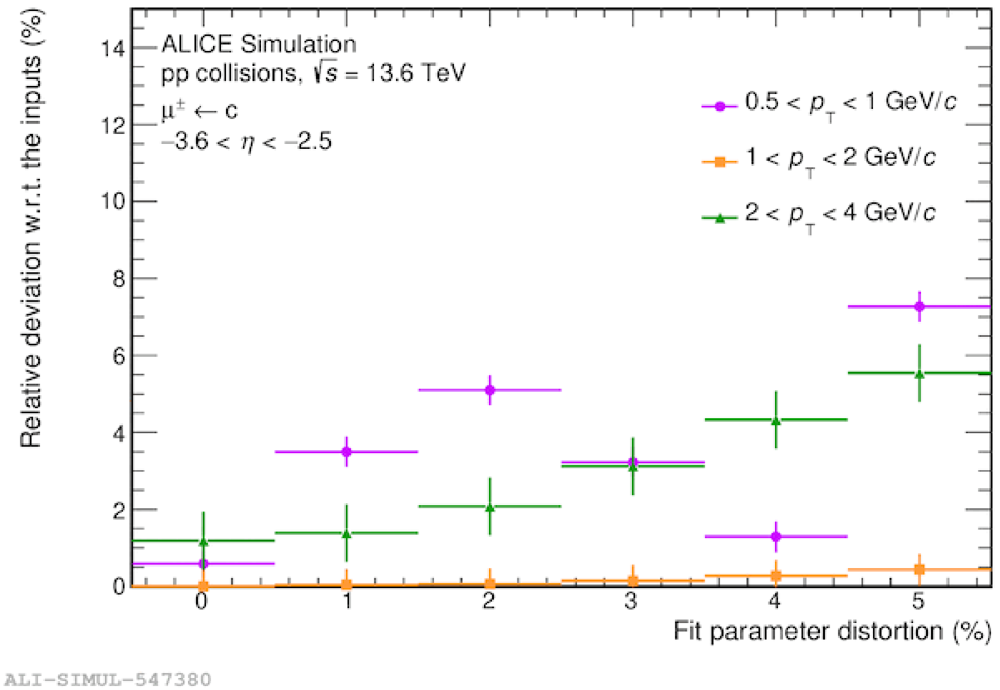

- $\mu \leftarrow c$ and $\mu \leftarrow b$ can be measured separately in the semimuonic channel at forward rapidity in pp collisions at $\sqrt{s}$ = 13.6 TeV with the MFT coupled with the muon spectrometer, down to about 0.5 GeV/*c* and 2 GeV/*c* for charm and beauty, respectively